Optimizing the Tracking Efficiency for Cosmic Ray Muon Tomography

LA-UR-06-7556

J.A. Green, C. Alexander, T. Asaki, J. Bacon, G. Blanpied, K. Borozdin, A. Canabal-Rey, M. Cannon, R. Chartrand, D. Clark, C. Espinoza, E. Figueroa, A. Fraser, M. Galassi, J. Gomez, J. Gonzales, A. Green, N. Hengartner, G. Hogan, A. Klimenko, P. McGaughey, G. McGregor, J. Medina, C. Morris, K. Mosher, C. Orum, F. Pazuchanics, W. Priedhorsky, A. Sanchez, A. Saunders, R. Schirato, L. Schultz, M. Sossong, M. Sottile, J. Tenbrink, R. Van de Water., K. Vixie, B. Wohlberg.

Abstract– **We have built a detector capable of locating high Z objects in the sampling (middle) region of the detector. As atomic number increases, radiation length rapidly decreases, yielding larger variance in scattering angle. Cosmic ray muon tomography works by tracking muons above the sampling region, and tracking them below the region as well. The difference between the two trajectories yield information, via the muon scattering variance, of the materials contained within the sampling region[1]. One of most important aspects of cosmic ray tomography is minimizing exposure time. The cosmic ray flux is about 1/cm^2/min, and the goal is to use them for detecting high-density materials as quickly as possible. This involves using all of the information possible to reconstruct tracks with redundant detectors. Detector scattering residuals yield a low precision measurement of muon energy. Knowing the rough energy of an incoming particle will yield more precisely the expected scattering variance (currently the expectation value of ~3GeV is used).**

I. Introduction

The muon tomography collaboration was created in 2001 to help address the problem of nuclear smuggling in a way that does not involve additional dose to occupants in a vehicle, and takes full advantage of the highly penetrating spectrum of cosmic ray muons.

When a charged cosmic ray particle (consisting of mostly electrons and muons at sea level) interacts with matter, it undergoes multiple coulomb scattering with nuclei. The small-angle scattering is described by a Gaussian distribution with a width, θ_0, of

$$\theta_0 = \frac{13.6}{\beta cp}\sqrt{x/X_0}\left[1+0.038\ln\left(x/X_0\right)\right],$$

where βc is the velocity of the incident particle, p is its momentum, x is the material depth, and X_0 is the radiation length of the material[2]. As atomic number increases, radiation length rapidly decreases, yielding larger variance in scattering angle.

Cosmic ray muon tomography works by tracking muons above and below the sampling region. Fig. 1 shows the apparatus built for this purpose. The difference between the two trajectories will yield information, via the muon scattering variance, of the materials contained within the sampling region. An important aspect of cosmic ray tomography is minimizing exposure time.

There are various techniques that will be discussed which work towards the goal of maximizing the efficiency of cosmic ray tracking. The cosmic ray flux is about 1/cm^2/min, and the goal is to use them for detecting high-density materials in a timely fashion. This involves using all of the information possible to reconstruct tracks with redundant detectors. Drift tubes usually require some fast-timing (conventionally PMT "paddles" or a beam-timing signal) to help determine the time that the particle passed through the drift tubes. The reference time and the time of the first hit is needed to compute the distance of closest approach to the anode wire within each hit tube. An alternative approach is discussed which uses the full set of drift tubes and all of the hits that a given charged particle produces in the system.

Fig. 1 The 20' tall Large Muon Tracker (taken October 2006), a sub-scale prototype built at Los Alamos National Laboratory, will vet the detector technology needed to field a full scale device. Overlapping X and Y detector planes are used to get the precise positions of the muon tracks above and below the sampling region. Also shown are the new redundant detector planes to improve tracking efficiency & quality.

Detector scattering residuals yield a low precision measurement of muon energy. Knowing the rough energy of

This work has been supported by Los Alamos National Laboratory, DARPA (defense advanced research projects agency), Department of Energy (NA-22 office), and the Department of Homeland Security (domestic nuclear detection office).

an incoming particle will yield more precisely the expected scattering variance (currently the expectation value of ~3GeV is used in the above equation). Though energy estimation is considered by the muon tomography collaboration, it is out of the scope of this discussion.

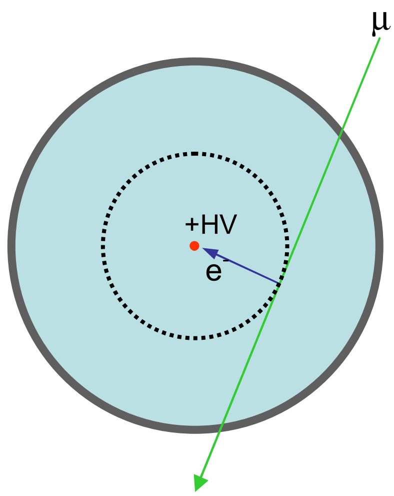

Fig. 2 Charged particle moving through a drift tube in the system. The dotted line shows the radius of closest approach to the anode wire. This radius is usually determined by the time it takes for the nearest liberated electrons to drift to the anode wire.

II. Detector Design and Construction

The large Muon tracker (LMT) consists of 6 top and 6 bottom planes of drift tube detectors for each X and Y dimension (total of 24 planes) on a frame which is flexible in design to allow for future changes (Fig. 1). In this context, a plane is defined to be a row of drift tubes at the same vertical (Z) location. The space between the top and bottom sections is about 1.5 meters allowing for a generous sampling region. Each pair of drift tube planes is tied together as close-packed cylinders in groups of 16 drift tube detectors for mechanical stability, mobility, and ease of electronics readout. The weight of a 16 tube module is approximately 28kg (see Fig. 3). This also means that each module is a part of 2 adjacent geometric planes, 8 channels each. The modules are installed onto the detector frame nested side-by-side in layers labeled as 1X, 1Y for the lowest pair of X and Y planes on up to 6X, 6Y for the upper X and Y planes.

The drift tubes were selected as a compromise between geometric efficiency, strength, multiple event rate, vertical clearance, and convenience of handling. The aluminum tubes were acquired (mostly) from Alcoaa corporation. The dimensions selected are 5.08cm (2”) OD (outer diameter), 0.0889cm (0.035”) thickness, and 3.65m (12’) long. The Al wall thickness of results in 96.5% geometric efficiency per plane. When glued together into a “module”, the combined strength of the arrangement is stronger than the sum of individual aluminum tubes. Each tube has an anode wire strung down the middle consisting of 20 micrometer Au-coated tungsten at 50 gram tension. The expected maximum catenary (wire sag) displacement is computed to be 200 micrometers.

Each anode wire is read out individually with a coupling capacitor → pre-amp → discriminator → ECL signal cable → time-to-digital (TDC) converter on a VME crate. This allows time to be readout of the hits on the wire. Each wire is read out on one side only (the front) of the detector. Hence, the only information about a hit is channel number and time. No information about where along the tube was hit is provided directly, but it is obtained from a track fitting.

Each 16 channel module provides a single “fast-OR” trigger signal, which is daisy-chained with BNC cables across the modules of a layer of detectors. The trigger signal is constructed from a coincidence of 2 microsecond gates (to allow for differing drift times to the anode wires) from layers 1X,Y & 3X,Y & 4X,Y & 6X,Y. Each of the individual fast-OR signals is fed to a separate TDC channel as diagnostics. To assist in the conversion of drift time to drift distance, a $2m^2$ scintillator paddle, instrumented by 4 PMTs and located below the lowest layer of drift tubes, is also read-out to a TDC, though it is not part of the hardware trigger decision. The PMT signal provides the ultimate “time zero” (or t_0) needed to determine the drift time and subsequent conversion to drift radius. Time zero can also be fitted using a least-squares method to remove the dependence on the PMT for timing and tracking.

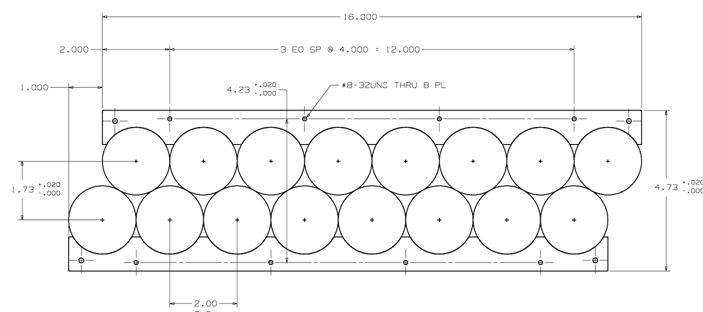

Fig. 3 Front view of an LMT drift tube module. Drift tubes are 12' x 2" with HV anode wire place in the center. Dimensions on diagram in inches.

III. Track Reconstruction

Because of the geometry of the detector, X and Y tracks are fitted separately (with Z as the dependent variable) to find a slope and intercept for each dimension. Together, these yield the 3D trajectory of the muon through the top and bottom regions. For reconstruction of scenes in the sampling region, top and bottom tracks are fitted separately, but for calibration top and bottom tracks are combined to better inform the fine positions and rotations of the drift tube anode wires.

For each hit drift tube, only the radius of closest approach (see Fig. 2) is available. The “straw man” version of the tracking is such that one and only one hit is registered per plane to simplify the tracking algorithm. In addition, only tracks that pass through the $2m^2$ scintillator paddle below layer 1X are used to facilitate the drift time conversion. Clearly, this is a severe limit to the tracking efficiency of the LMT, but was convenient for the initial work. Much higher-efficiency algorithms are currently being studied to push the feasibility of the apparatus. Hit filtering prior to track fitting and the fitting of "time zero" to allow conversion of drift time to a drift radius for each hit tube has also been studied. This last step is vital in removing the need for the track to pass through scintillator paddles. Computation of the drift radius is done with a calibrated conversion of drift time to radius. The least squares method is used to fit 3D tracks through the top and bottom portions of the detector separately.

A. Segment-based Hit Filter

One or more hits on each layer (pair of nested planes) of the system will produce a trigger. The data for this trigger is time and channel number which is then converted to drift radius and calibrated wire position. The times are used to place the hits into a window of 2 microseconds (approximately the maximum drift time). These hits are selected using a two-point line segment algorithm, which works as follows:

1. Construct a line segment between all pairs of hits which a) would belong to the same track, b) are members of a different layer (plane pair).
2. Compute for each segment a) slope, b) intercept, c) compute median of slopes and intercepts
3. Select segments which agree with the median slope and intercept values within a tolerance of 0.15 for slope and 10 cm for intercept
4. Accept only hits associated with one or more selected segments.

The purpose of this algorithm is to remove hits which are unlikely to contribute to a track due to noise. The selected segments are selected for their compatibility with the most prevalent straight trajectory. The number of combinations of segments is no more than about 20 when fitting top and bottom tracks separately.

B. Wire position and time of flight (TOF) corrections

Prior to tracking, all corrections are applied to wire positions and rotations. We assume that rotations are small, so knowledge of track positions to ~5cm is sufficient to apply the corrections. For this, track fits are done which ignore the drift radius. This gets the tracks well enough to approximate the position of the hit along the length of the drift tube. This is used for rotation, time of flight, and catenary (wire sag) corrections. For TOF, the travel time of the through-going particle is estimated to within a few cm, and the propagation time down the anode wire is also added. Cable propagation is ignored since all signal cables are length matched to < 2 cm. Numerous correction values for each wire's position and rotation relative to nominal are acquired through the calibration process.

C. Time-zero Fitter

Time-zero, t_0, is the reference time needed to compute the drift radius of each hit drift tube in an event (see Fig. 4). It is assumed that the same t_0 applies for all hits in an event (after applying TOF corrections explained above). For each trial value of t_0, a standard least squares routine is used to compute track parameters, and the associated total χ^2 for all tracks. The value of t_0 is allowed to vary in an interval from the time of the first hit until the median of the groups of hits in the event. The starting value is the time of the first hit, and a modified grid search is used to find the t_0 associated with the minimum χ^2. Assuming the shape of χ^2 w.r.t. t_0 to be convex (open upwards), a parabolic fit is used to get the final t_0 value of and its error estimate. A typical number of iterations for a t_0 fit is 20, with the final value of χ^2 /DF at about the right place (see Fig. 5). This includes coarse (100ns interval), medium (10ns), and fine (~1ns). Typical parabolic errors are on the order of 5ns (see Fig. 6).

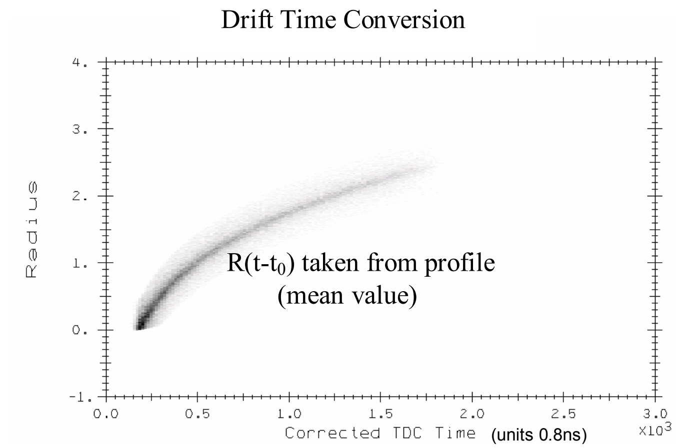

Fig. 4 Radius in centimeters from anode wire (Y-axis) versus drift time (in units of 0.8 ns) . In order for the drift conversion to take place, the base reference time must be known. The corresponding profile histogram is used to compute the time-to-distance conversion table for each 32-tube group of drift tubes.

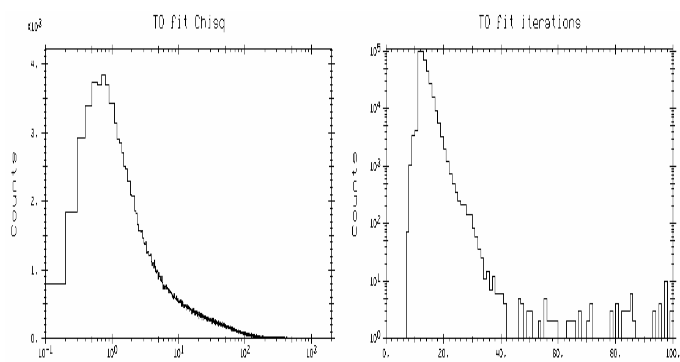

Fig. 5 Chi-square per degree of freedom (peak near 1), and number of iterations needed to locate time zero.

D. Geometric and Tracking Efficiency

The geometric inefficiency due to thickness of the aluminum tubing is 0.0889cm/2.54cm = 0.035 (or an efficiency of 96.5%). The measured efficiency using cosmic ray tracks agrees within statistical error. The efficiency of a layer of 2 planes of nested tubes is measured to be 99.5% also consistent with geometric arguments. Hence, an expected efficiency of ~94% results in requiring 1 or more hits in every pair of planes (12 pairs or layers).

Overall tracking efficiency is improved by using the segment-based hit filter as well as the time-zero fitter as opposed to requiring a PMT hit (see Fig. 7).

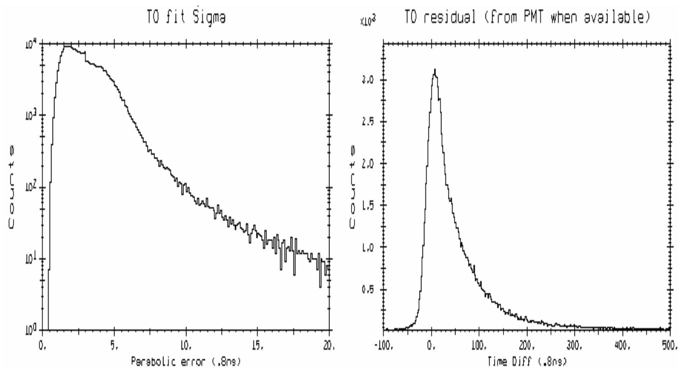

Fig. 6 Error (parabolic) of time zero fit in units of 0.8 ns, and on the right is a comparison of fitted time zero (also in units of .8 ns) to scintillator PMT when the track passes through the scintillator below.

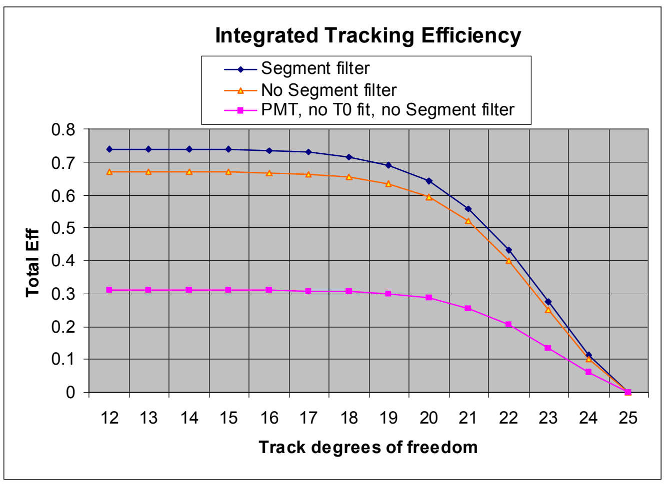

Fig. 7 Comparison of overall efficiency of tracking versus track degrees of freedom in three cases. The least efficient is the requirement of a PMT hit. With time-zero fitting, it is possible to reconstruct many more tracks with lower cost.

IV. Calibration

In order to establish tracks with as high resolution as possible, the geometric positions, rotations, and time-to-radius conversion of each drift tube must be established. Following detector installation onto the large muon tracker, these measurements are done by hand with standard techniques using tape measure, plumb bob, and carpenter's square to the nearest few mm to give subsequent calibration a starting point. What follows is measurement of tube positions, rotations and time-to-distance conversions via cosmic rays.

The overall calibration procedure is iterative as one might expect. Initially, the time-to-distance conversion is unknown, so using the assumption of constant flux as a function of distance from the anode wire, the integral of the TDC spectrum is assumed proportional to the distance that the closest electron travels. The maximum value (plateau) of the integral is then set to the inner radius of the tube wall. From the known initial positions of the drift tubes, we can now begin taking track data and reconstructing crude tracks through the LMT.

The first stage is to measure the average horizontal position of the first wire of each drift tube plane. It is initially assumed that the interval between drift tubes (anode wires) is assumed to be a constant (2"=5.08cm) and that there are no rotations to be considered. Rotations are a fine adjustment, since an attempt is made to place drift tube modules in rectilinear (making orthogonal planes) fashion.

Track residual distributions are used directly to compute new wire positions in which track quality cuts are: minimum number of degrees of freedom, $\chi^2/DF < 2$, and slope cuts. The horizontal residual, $R_H = X_{point} - X_{track}$, where X_{track} is the horizontal position of the track at the current Z position of the anode wire, and X_{point} is the current horizontal position of the anode wire added (or subtracted depending on the track fit) to the radius of closest approach of the hit (using drift time conversion) also projected to the Z location of the anode wire. The point in question is left out of the track fit. Each track informs the residuals of its constituent points in this way. The goal of calibration is to drive the residuals to zero, and to achieve as narrow as possible a residual distribution. Similarly, $R_V = Z_{wire} - Z_{track}$ is the corresponding vertical residual used to measure the position of the detectors in the Z coordinate, and $Z_{track} = (X_{track} - b)/m$ from the intercept (b) and slope (m) of the fitted track, and Z_{wire} the current known vertical location of the wire. The track slope is required to be >= 0.15 for vertical corrections and < 0.10 for horizontal corrections, where slope zero corresponds to a vertical track. In a similar way, vertical fine tuning of the plane position is done assuming there is no tilt of the tubes. The horizontal & vertical plane positions are iterated until results are stable (several iterations are needed). Next, horizontal & vertical positions of individual tubes are computed and iterated also using the residual technique. Horizontal rotations and tilts (vertical rotations) are then found by measuring track residuals as a function of distance along a tube and using linear regression to get the slope and intercept of each tube. The improved detector positions are now able to inform the drift time spectra by direct measurement. This is the last step in the list of calibration constants. Except for the 0th – order overall plane positions, the calibration constants are iterated approximately 10 times over about 1 day of cosmic ray data with no objects in the scanning region of the LMT. Once the constants are clearly starting to converge, the calibration loop is set onto an automatic mode since changes in the parameters will be small and are expected to converge.

References

[1] K. Borozdin *et al.*, "Radiographic Imaging with Cosmic Ray Muons," Nature, 422, p.277 (2003).

[2] Review of Particle Physics, S. Eidelman *et al.*, Phys. Lett B 592, 1 (2004).